
MASTER THESIS

# Creation and evaluation of a realistically shaped EIT tank

*Author:*
Eric Waldburger
Mat. Nr.: 321292

*Examiners:*
Prof. Dr. Benjamin Blankertz
Prof. Dr. Klaus-Robert Müller

*Supervisor:*
Nils Harmening

*A thesis submitted in fulfillment of the requirements*
*for the degree of Master of Science*

*in*

Computer Science

Berlin,
December 17, 2024

## Abstract

This thesis tries to validate the a 3D printed head phantom for EIT experiments and aims to increase the accuracy of it by including a conductive cortex mimicking the conductivity of the brain. The cortex was designed and integrated into the existing model using Protopasta conductive PLA as a base.
Experimental measurement were taken with varying frequencies and amplitude and compared against simulations created with the python based Pyreite. The resulting correlations were showing hardware limitations and emphasizing the importance of preparing phantoms for multifrequency EIT measurements. Despite some shortcomings it concludes that 3D printed conductive materials could be used to validate EIT systems.



## Zusammenfassung

Diese These beschäftigt sich mit der Validierung eines 3D gedruckten EIT-Kopf-Phantomes und hat sich als Ziel gesetzt die Genauigkeit dessen zu erhöhen. Dies soll durch die Erweiterung des Phantoms um einen Cortex geschehen, welcher versucht die Leitfähigkeit eines Gehirnes möglichst realitätsnah nachzuahmen. Dies soll auf Basis von leitfähigem PLA von Protopasta geschehen
Es wurden mehrere experimentelle Messungen mit verschiedenen Frequenzen und Amplituden durchgeführt, welche Simulierten Daten verglichen werden. Diese wurden mit dem Python Framework Pyreite erstellt. Die resultierenden Korrelationen deuten zeigen Limitierungen in der Hardware auf und zeigen, wie wichtig es ist Phantome auf die Messungen mit verschiedenen Frequenzen vorzubereiten. Trotz einiger Probleme wird gezeigt, dass leitfähiges PLA trotzdem zum Validieren von EIT Systemen verwendet werden kann.

# Acknowledgements

I again want to thank Nils Harmening keeping up and supporting me for a long time. Additional thanks to Daniel Miklody for helping me setting up the experiment runs and for debugging his EIT-Board with me. Finally I want to thank Prof. Blankertz for the chance to write my thesis in his field and introducing me to BCI years aga in a bachelor project.

# Contents

# List of Figures

# List of Tables

## Abbreviations

| | |
|---|---|
| EIT | **E**lectrical **I**mpedance **T**omography |
| EEG | **E**lectro**E**ncephalo**G**raphy |
| FEM | **F**inite **E**lement **M**ethod |
| PU | **P**oly**U**rethane |
| PLA | **P**oly**L**actid **A**cid – common plastic used for printing 3D Models |

## Relevant Terminology

| | |
|---|---|
| PHANTOM | Model of a desired structure used to gather reliable data |
| MESH | 3D model constructed out of vertices, edges and faces. |
| VERTEX | Single point in a 3D structure |
| EDGE | Connection between 2 vertices |
| FACE | A planar surface that fills the space between multiple edges |
| INFILL | Defines how a 3D printer should fill the inside of model |
| FLOW RATE | The amount of material extruded trough the nozzle |
| RAFT | Support structure for 3D printing. The printer will place some layers below the model that work as a foundation. |

## Important Units

| | |
|---|---|
| Ω*m, Ω*cm | Resistivity |
| S/m, S/cm | Conductivity, inverse of the resistivity |
| ρ | Symbol for resistivity |

# 1 Chapter - Introduction

## 1.1 Motivation

Electroencephalography (EEG) utilities electrodes placed on the scalp to measure voltage fluctuations caused by neuronal activity. These values are passed to an algorithm which tries to localize the source of the signal. This is very difficult because the signal itself is weak and has to pass through different layers of varying conductivity. Only the range these conductivities can have is known but rarely the specific value for this subject. Which makes it harder to narrow down the source location. If these conductivities were known the accuracy of the EEG could be increased.
This is where area where EIT could be used to improve the overall result. It works by injecting a small current into the head and measuring the voltage responses on the outside electrodes. This is repeated for all pairwise combinations to gather as much data as possible and reveal the underlaying conductivity distribution. This is known as solving the inverse problem. Which is ill-posed because there could be more than one possible solution and any error on the electrodes could lead to a significant error in the reconstruction. To minimize the risk of errors, the hardware and software is often validated with phantoms. Which are tools designed to have fixed characteristics that will always return similar results when measured. So it would be possible to find differences when measuring them with different devices or test how reliable a single device is after multiple measurements.
In this thesis we wanted to test if the phantom from (Avery J. a., 2017) can be used with our equipment and if its accuracy can increased with a cortex model.

## 1.2 Phantoms

A phantom is a physical object or a simulation with specific characteristics that are similar to the item under analysis. It is used to validate hardware and software by offering a controllable and repeatable test environment. Which in turn helps to create robust algorithms that include and / or minimize noise from the hardware, find and eliminate noise sources in the setup. It also provides the chance to test the reliability of the hardware over

multiple experiment. Phantoms, especially physical ones can often be considered a step between simulations and live experiments.

The following section will summarize the paper that was the basis for this thesis as we wanted to replicate their tank and test the results with a 3D printed conductive cortex.

### 1.2.1 Reproducible 3D printed head tanks for electrical impedance tomography with realistic shape and conductivity distribution (Avery, Aristovich, Low, & Holder, 2017)

In this work, the authors wanted to create an EIT phantom that can be easily recreated, is very similar shaped to a real head. It should require minimal modifications by researchers to reduce the risk of inconsistencies between multiple models. Lastly the phantom had to be reusable over a long period.

**Model:**

The phantom was designed to be printed on a 3D printer with non-conductive PLA and electrodes made from stainless steel 316 because of its high corrosion resistance. The form of the tank and skull were the result of analyzing a number of high-resolution CT and MRI scans that allowed a retrieval of the different skull segments. Only the part from the "inion-nasion line" upwards was chosen because this area includes most of the brain. Facial features and the neck were excluded as much as possible because the effect these parts have on EIT is still not fully known. (Tidswell AT, 2003). The next step was to prepare the meshes by "smoothing[1]" the surface and removing artifacts. The tank was scaled up by 10% to become an outer limit and create space for the skull to be inserted later and holes where added to hold 33 electrodes. These were positioned according to the positions in Fig 1 in (Tom Tidswell, 2001). Four electrodes had to be moved to the closest 10-10 or 10-5 extensions. There was no specific reason mentioned why the electrodes were moved.

To ensure the accuracy of the print the tank was scanned with an optical scanner and compared to the original CAD model. The measured deviation was evenly distributed and in the range of 0.21mm +- 0.101mm. See Fig. 1 for our print of the phantom.

**Conductivity:**

To model the skull conductivity with non-conductive material, holes with specific diameters and distances were added for the saline solution in the tank to pass through the skull. The resistivity can be estimated using:

$$\rho_{eff} \approx \frac{A_{total}}{A_{saline}} \rho_{saline} \qquad \textbf{(1)}$$

This equation was used to calculate the resistivity of the skull. Because the holes are filled with saline solution and the used PLA is an insulator, the relation between these areas can be used to estimate the resistivity. To verify this, the phantom in Fig. 2a was

[1] Simplifying the structure by combining nodes and vertices which can prevent some printing artifacts

built. It was a tank with 2 electrodes on each side and a plate in the middle with a specific hole distribution. The difference between the measured resistivity and the targeted was smaller than 3%. They spaced the holes 5 mm apart and found that only diameters in between 1 mm and 2.5 mm would work for them. The 3D printer had problems printing

the holes consistently with a diameter outside this range. The resulting values are shown in Fig. 2b.

**Fig. 1:** Complete phantom with tank, skull, electrodes and support to hold the skull in place.

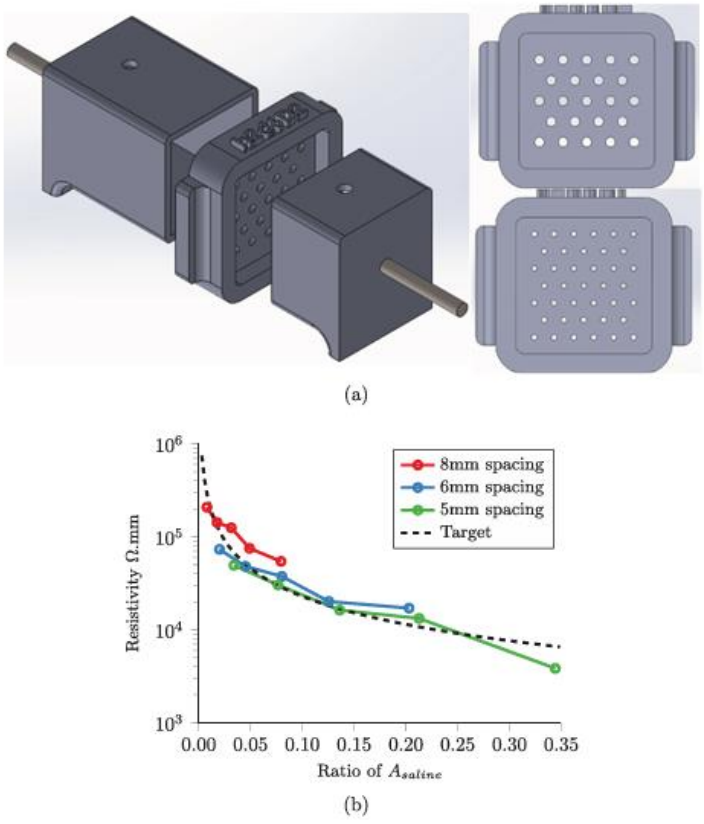


**Fig. 2: a)** Shows the phantom used to test the different hole configurations. **b)** Shows the resulting relationship between the effective resistivity and the spacing of the holes.[2]

The conductivity of the skull was based on the findings from (Tang, 2008) shown in Tab. 1. Analyzing the values for the bones they came to the conclusion that the further a point

is from the top of the head to the front or back. Then the conductivity would increase up to 87% and decrease on the sides up to 32%. This led to the following linear combination:

$$\sigma_{xy} = \sigma_0(1 + 0.87\frac{x}{x\_max} - 0.32\frac{y}{y\_max}) \quad (2)$$

**Tab. 1:** Resistivity values for a human skull [3]

| Position | Type of bone | Resistivity (Ω*m) |
|---|---|---|
| Frontal Bone, Occipital Bone | Standard Tri-layer | 79.43 |
| Parietal Bone | Quasi-tri-layer | 144.71 |
| Sphenoid Bone, Temporal Bone | Quasi-compact | 192.24 |
| Parietotemporal Suture | Squamous Suture | 127.47 |
| Lamboid Suture, Coronal Suture, Sagittal Suture | Dentate Suture | 57.82 |

Both equations were used to calculate the diameter of the holes on the skull with a fixed spacing of 5mm between them.

**Test run:**

For the data collection the tank was filled with 0.2% saline solution and the "ScouseTom" system, described in (Avery J. a., 2017), was used. A total of 31 pairwise injections with a length of 75 ms over 20 frames were performed. The injected current had an amplitude of 200 µA at 1.4 kHz. This was done with and without the skull and the results were averaged for each of those types. The collected boundary voltages were compared to FEMs generated on the CAD model with the error being the absolute difference between voltages and afterwards condensed into the mean and standard deviation.

The correlation between the simulations and the experiments voltages was very high with $R^2$=0.997 and an error around 0.215 mV for most channels and 0.513 mV for the worst.

To compare the results, the error was calculated as the absolute voltage difference between the experiment and the simulation. Which was 4.87% without the skull and 4.50% with the skull.

**Discussion:**

Their tests revealed that the use of a 3D scanner allowed the comparison between the printed model and the original mesh and that the accuracy of the 3D printer was in fact a limiting factor. While most printing artefacts had no influence on the final result, some could prevent electrodes from fitting into the tank and cause them to be misaligned. Artifacts on the skull could change the direction and or diameter of the holes which can cause problems as the resistivity approximation requires the holes to be aligned with the electrodes. They proposed that creating the holes in the skull, perpendicular to the scalp surface instead of the skull itself could decrease this error. The electrodes at the top of the

[2] Fig. 1 from (Avery, Aristovich, Low, & Holder, 2017)

[3] Adapted from (Li, et al., 2014), based on (Tang, 2008)

tank were also producing a higher error than the ones at the bottom which led them to think it could be a change in the saline level of the tank.
They also mentioned that the use of a single saline solution is a common simplification in these phantoms but is less realistic than the use of isotropic layers in existing methods and that the skull was designed for 1 kHz experiments and based on the work fromm (Tang, 2008) and could require changes for experiments with other frequencies.

**Conclusion:**
They concluded that they succeeded in creating a phantom that was easier to reproduce than earlier mold based phantoms by allowing all the parts to be directly created on a 3D printer. The accuracy of printer seems to be very important since printing artifacts and, misaligned electrodes could cause tortuosity effects which caused the error to go up to 5%.

## 1.3 Cortex phantom

Most EIT phantom tanks were designed with the focus on reconstructing an image based on the conductivity of the item in the tank (Yu, 2006) (Zhang, et al., 2017). We wanted to use the tank with a cortex phantom to try and create another option besides simulations to validate algorithms and hardware. For this we wanted to create a cortex model that has the average conductivity of the brain, a similar shape and is durable. It should also not degrade over time. The target conductivity was based on the discoveries by (McCann H, 2019) and (Jun Ogata, 1973). We used the weighted average of the values for gray and white matter and got 270,27 Ω*cm as our target resistivity respectively 0,37S/cm as target conductivity.
The next step was to find materials for the cortex that would be close to the correct conductivity. PU was one possibility since it can be made conductive with additives. We chose single-, multiwalled carbon nanotubes (SWCNTS, MWCNTS) from **Fig. 3** as these had a similar conductivity to the human brain. Other options were Carbon Black although it itself had no value in this table, it was used together with carbon nanotubes (Melo, 2023), and silver nanoparticles as another alternative (Saeid Mehvari, 2023). The problem with these PU based solutions was that most additives were very expensive and it would be quite hard to ensure a uniform distribution of nanoparticles during mixing and pouring. A support agent from TUBALL[4] told us that to guarantee a good distribution of the nanotubes we would have to use a lab stirrer with specific impeller blades. Equipment

[4] Link to homepage: https://tuball.com/de

we did not have available to us. We would also have to perform a series of tests to find the correct percentage for our setup.
That is why we decided to work with conductive PLA as this would allow the cortex to be printed with a 3D printer and could easily be reproduced and modified.

**Table 1** Conductive polyurethane composites used for various applications

| S.No | Conductive material used (wt%) | Conductivity of the composite(S/cm) | Demonstrated/suggested application | References |
|---|---|---|---|---|
| 1 | PAni (30 wt%) | $4 \times 10^{-4}$ | – | [20, 21] |
| 2 | PAni (34 wt%) | $8 \times 10^{-2}$ | Antistatic | [23] |
| 3 | PAni (1–75 wt%) | $3.3 \times 10^{-1}$ | Antistatic | [26] |
| 4 | PAni (10 wt%) | $1.7 \times 10^{-5}$–$2.4 \times 10^{-5}$ | Fuel cells, dialysis | [28] |
| 5 | SPAni | $1.1 \times 10^{-2}$–$2.2 \times 10^{-5}$ | – | [31] |
| 6 | PAni (30 wt%) | $1.7 \times 10^{-6}$–$1.5 \times 10^{-2}$ | – | [29] |
| 7 | PAni (10.6–26.4 wt%) | $1 \times 10^{-8}$ | Antistatic | [30, 35] |
| 8 | PAni (2 wt%) | $1 \times 10^{-4}$ | Corrosion protection | [36] |
| 9 | PTh | $10^{-4}$–$10^{-2}$ | – | [42] |
| 10 | PPy | $10^{-7}$–$10^{-2}$ | Pressure sensing | [38–40, 96] |
| 11 | PPy-30 wt% | $2.6 \times 10^{-1}$ | Sensors, packaging materials | [44] |
| 12 | PPV | – | Photoelectrochemical cells | [92–94] |
| 13 | Carbon black | – | VOC sensor, shape-memory | [71–73, 95] |
| 14 | SWCNTS (3 wt%) | $5.9 \times 10^{-3}$ | Shape-memory | [84] |
| 15 | MWCNTS (10 %) | 5.3 | Flexible electronic displays | [101] |
| 16 | SWNTs (5 wt%) | – | Microwave absorption | [68, 69] |
| 17 | Opt. active MWCNTs (0.5 wt%) | $1.58 \times 10^{-3}$ | Intelligent textiles | [65] |
| 18 | MWCNTs (5 wt%) | $1 \times 10^{-3}$ | Shape-memory | [82] |
| 19 | SWCNT + PPy | $9.8 \times 10^{-3}$ | Shape-memory | [83, 84] |
| 20 | CNTs with azo ggroup | – | Photonic devices | [89] |
| 21 | CNTs with Ni–Fe nano | – | Removal of trichloro-ethylene | [91] |
| 22 | MWCNTs | – | Biomedical | [75–80] |
| 23 | Graphene (2 wt%) | $10^{-5}$, $10^{-8}$ | Various applications | [100, 101] |

**Fig. 3**: Overview of some additives used to make PU conductive [5]

[5] Table 1 from (Gurunathan, 2013)

# 2 Chapter – Methods

## 2.1 Materials

### 2.1.1 Tank phantom

We used the CAD models provided online[6] for the tank phantom described in 1.2.1 and imported them into IdeaMaker[7]. This software is used to create the instructions for the 3D printer by “slicing” the model into horizontal layers that the printing nozzle will follow and build the model layer by layer from the ground up. Additional settings for the print like the height of each layer, the printing speed, settings regarding the infill are also configured there. If there are parts of the model that have no direct connection to the ground they require support or the layers will fall down during the print. This can be seen in Fig. 4 b) where the yellow parts are required for the print but can be removed afterwards. IdeaMaker offers an “auto support” feature that will analyze the model and automatically create needed structure. This worked in prior prints so it was used again for the tank.

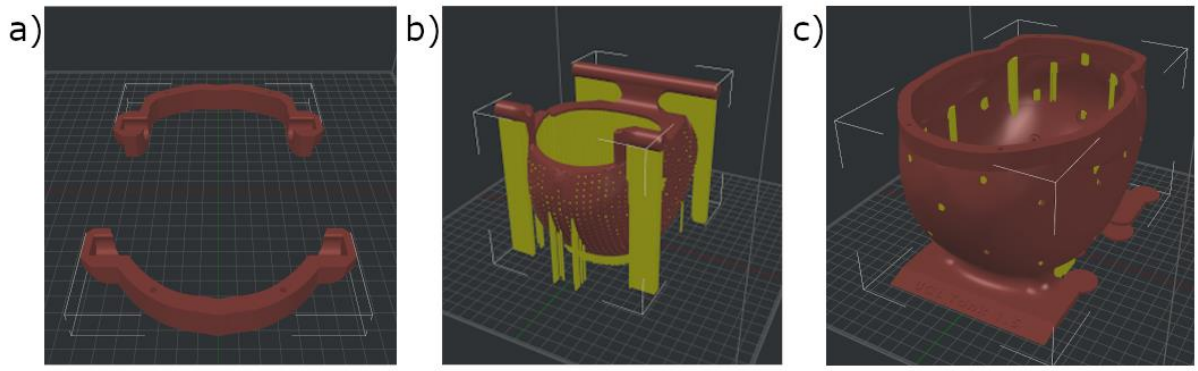


**Fig. 4:** The mesh for the tank imported into the slicer. Red is the actual mesh and yellow is support required for the print a) Holders for the skull b) Skull c) Tank

The print was performed on a Raise 3D Pro2 that has 2 extruders and should be able to work with 2 different types of plastics. We wanted to use Extrudr PLA NX2 for the model and specific support PLA that should be easier to remove. The printer had some problems

[6] Available here: https://github.com/EIT-team/Tanks/

[7] Slicer by Raise3D available here: https://www.ideamaker.io/features.html

with this approach. (Fig. 5) As a result we tried only using the Extrudr PLA and use sand-paper to clean the surface and remove printing artifacts.

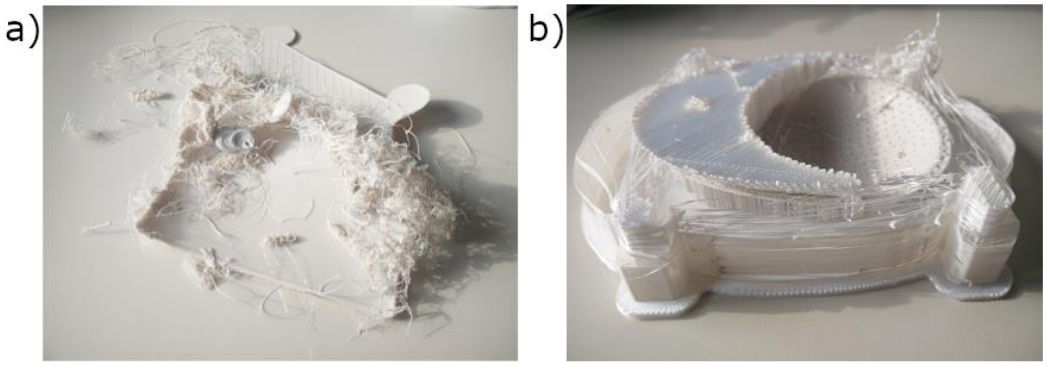


**Fig. 5:** Print errors with 2 extruders. a) Model didn't stick to the baseplate b) A nozzle was stopped printing because of a temperature drop ~ 15°C

The electrodes for the tank were ordered online from Hubs[8] and made with stainless steel 316 with the CAD files from the git repository. These were inserted into the tank and sealed with silicone. The inside of the tank had to be sealed to prevent water leaking. The assembled tank is shown in Fig. 1. An old cables used to connect to EEG-Caps was repurposed to connect the tank to our hardware. For this we cut of the cap connectors and soldered on some crocodile clamps. This way we could attach them to the outside electrodes of the phantom.

### 2.1.2 EIT Measurement device

The EIT measurement device was already designed Daniel Miklody in his master thesis (Miklody, 2014). It is a device that allows pairwise current injection with up to 64-channels, an amplitude in the range of 0-300 µA and frequency range of 0-10 MHz. The device is

[8] https://www.hubs.com/

placed in between the EEG amplifier and the cap and was controlled with MATLAB[9] over the serial port interface.

**Fig. 6:** EIT measurement device

### 2.1.3 Conductive PLA

Protopasta conductive PLA[10] was chosen as a conductive printing material as it was readily available at the time and the conductivity was “close” to that of the brain. In the documentation of the material the resistivity is given for the x-y axis with 19.2 Ω*cm and 33.6 Ω*cm along the z-axis for the lowest printing temperature of 210°C. Higher temperatures would lead to a better bond of the plastic which would then lower resistivity and were thus of no interest for us.
We thought about the difference of the axes and wanted to test if different infill percentages have an effect on the conductivity. As it would be hard to simulate results for a model that has an axis with double the resistance.
To test this we were printing sets of cubes with different infill percentages and chose “Honeycomb” as the general infill pattern. An exception was made for 100% infill with lines for the reason that 100% honeycomb infill had still empty spaces inside. (See Fig.

[9] Available here: https://mathworks.com/products/matlab.html

[10] Available here: https://proto-pasta.com/products/conductive-pla?variant=1265211476

7). Multiple cubes were printed for each configuration to have redundancy in case of printing errors.

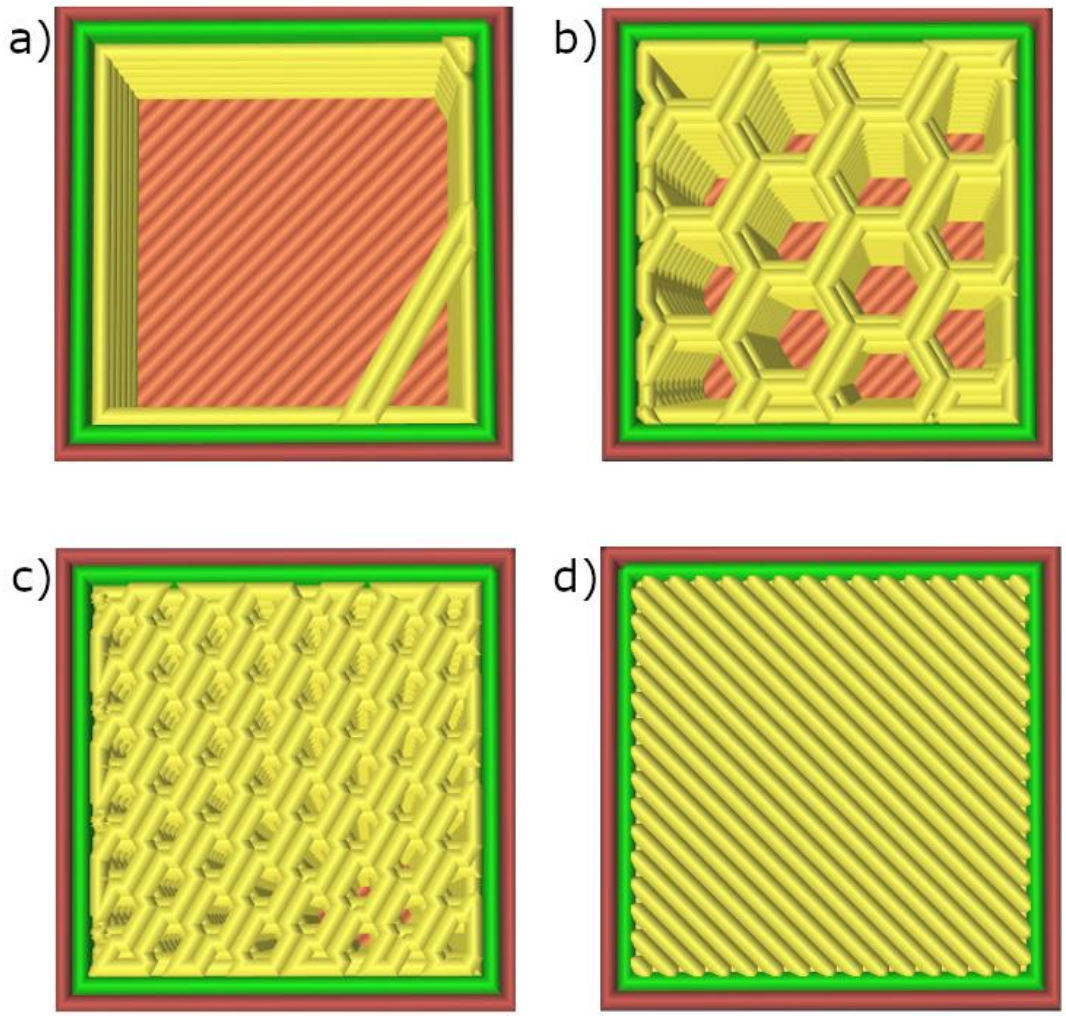


**Fig. 7:** Different examples for infill patterns used in the cubes. a-c) 5%, 50%, 100% honeycomb infill. d) 100% lines

### 2.1.4 Combining the tank with cortex model

We had a cortex scan available from a team member and decided to use this as the template for the experiment.

All the meshes from the tank phantom were imported into a Blender[11] project. The tank, skull and supports were arranged so that everything would be similar to the existing print. The next step was to import the scan and place it inside of the skull. We first only scaled it down to barely fit but decided on shrinking it further to give us the option of getting it into the skull and out again. That would allow the tank and skull to be reused with a

[11] Blender Available here: https://www.blender.org/, Project file here: https://tubcloud.tu-berlin.de/s/JDTp-bEmM5GKkyYc

different cortex. The opening in the skull still required us to remove some material with a saw and file to allow the insertion of the brain.
To keep the brain inside the skull without touching the sides two support structures were added. The T-shaped support parts required holes in the brain as these should not be conductive. But generating the holes was quite the challenge because the scan had a lot of problems with overlapping faces and faces with wrong orientations. This led to the slicer suddenly using the infill pattern for a part of the hole. We tried reducing the complexity of the mesh by merging close nodes, removing some faces, fixing the orientation of faulty ones but the mesh was too complex. The work required to fix everything wasn't worth it. In the end we decreased how far the support pole would go into the cortex. It was enough to keep the brain in place. The steps in blender are shown in Fig. 8 and the full assembly is shown in Fig. 9. To combat the buoyancy of the cortex a weight has to be placed on top of the support to keep it from floating during experimentation.

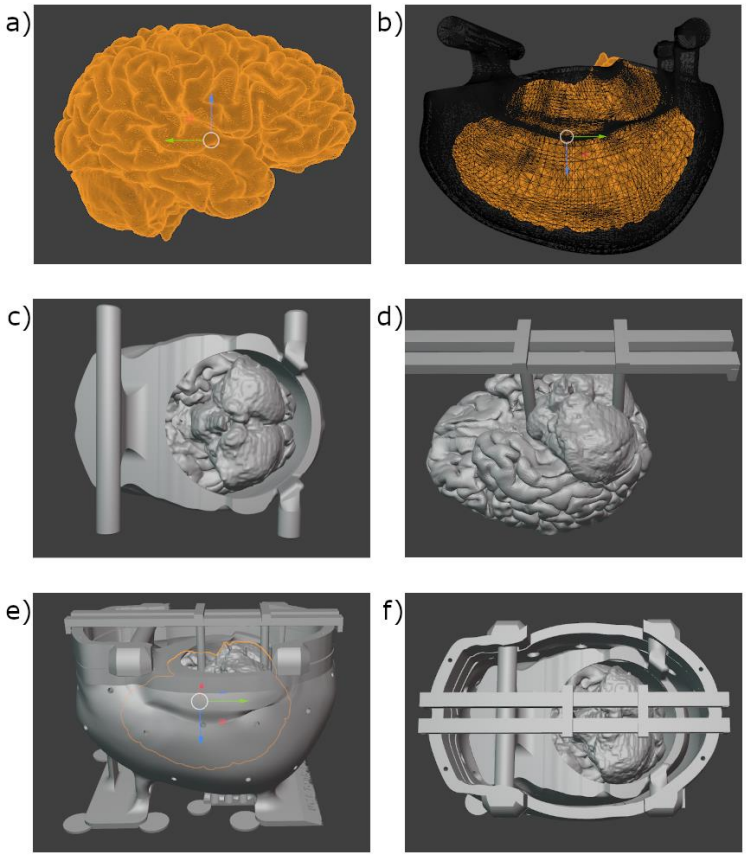


**Fig. 8:** Images from Blender. a) Cortex b-c) Cortex in skull d) Cortex with holders e-f) Tank phantom with cortex additions

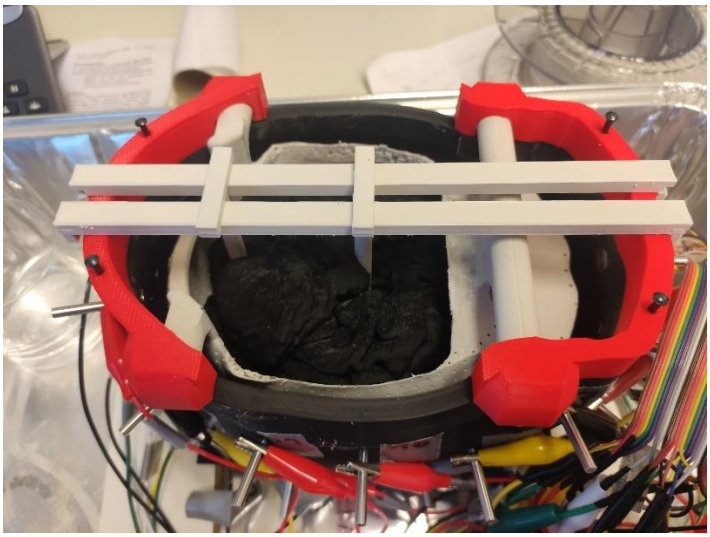

**Fig. 9:** Phantom with cortex

## 2.2 Methods

### 2.2.1 Conductivity measurement

Due to hardware limitation we had to use the 2 probe method (see Fig. 10a) to get the conductivity of our cubes. The method was compared with others by Khalid Inzamam

(Khalid, 2023) and is normally used for samples with a lower conductivity. This is because the contact resistance can be higher than the target resistance which would prevent us from getting an accurate result. Possible reasons for this contact resistance could be an uneven surface trapping air, oxidation of the material or other chemicals present on the surface.

$$\rho = R \cdot \frac{A}{l} \qquad (3)$$

We were using copper plates as electrodes and a multimeter to measure the resistance. Fig. 10b shows our setup. According to (3) the resistivity is the resistance multiplied with the contact area divided by the length of the sample. We chose the dimension of our cubes to be 1 cm so that $\rho = R$ so that it would be possible to directly get the results with a multimeter and not use up too much of the conductive PLA.

To decrease the contact resistance the sides of the cubes were sanded down to remove artifacts and flatten the layers. The sides were then cleaned with isopropyl alcohol and two opposing sides painted with a silver based paint to further minimize the resistance.

We tried to measure the resistivity without the silver paint but the results were highly dependent on the pressure used to press the copper plates onto the cube. The reading took sometimes longer than 15 minutes until it would slow down and finally stop at a

resistance value. With the silver paint the values were constant the moment a very low pressure was applied and did not change when the pressure was increased.

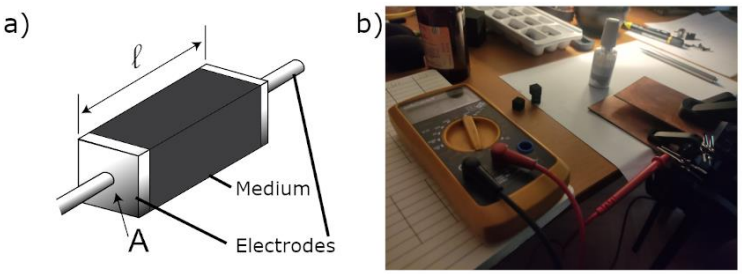


**Fig. 10:** a) Schematic two probe method setup[12] b) Our setup

### 2.2.2 EIT Experiments

We were using a setup with 32 electrodes and 1 ground electrode. They were labeled according to Fig. 11. Our toolchain to record the data consisted of the following elements:

- **Tank phantom**
- **EIT Measurement device:** Used to inject the current and pass the voltages on
- **BrainVision BrainAmp[13]:** Amplifies the voltages
- **PC:**
  - **BrainVision Recorder[14]**: Save the data to the disk
  - **MATLAB:** Controls the measurement device and when the recorder saves the data

Fig. 12 shows the full setup for measurements with an empty tank and Fig. 13 with skull, cortex and improvised weight to keep the cortex from floating.

[12] Adapted from Wikipedia: https://en.wikipedia.org/wiki/Electrical_resistivity_and_conductivity

[13] Available here: https://www.brainproducts.com/solutions/brainamp/

[14] Available here: https://www.brainproducts.com/downloads/recorder/

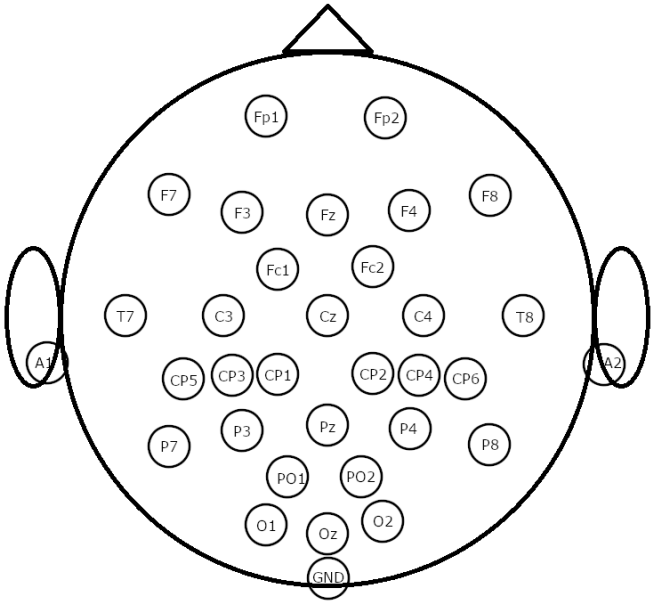


**Fig. 11:** Electrode labels used during the experiments. 32 electrodes for measuring and one ground.

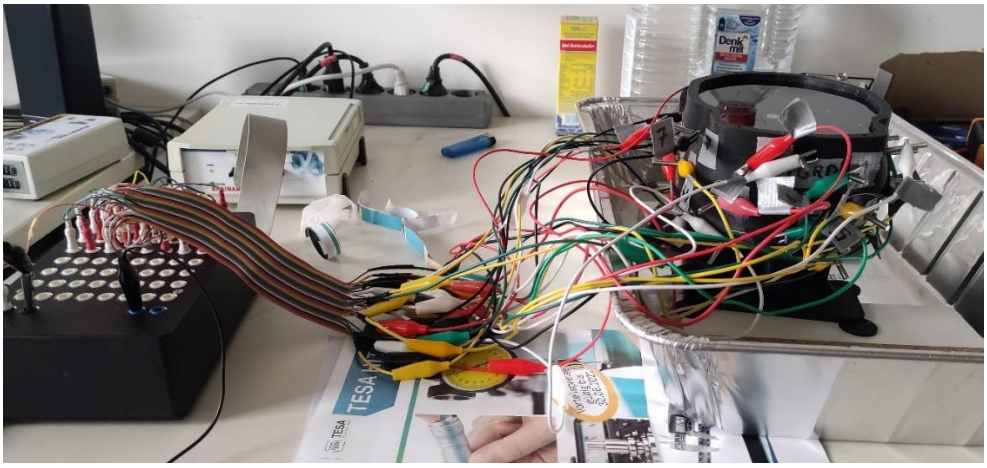

**Fig. 12:** Setup for EIT measurement without skull

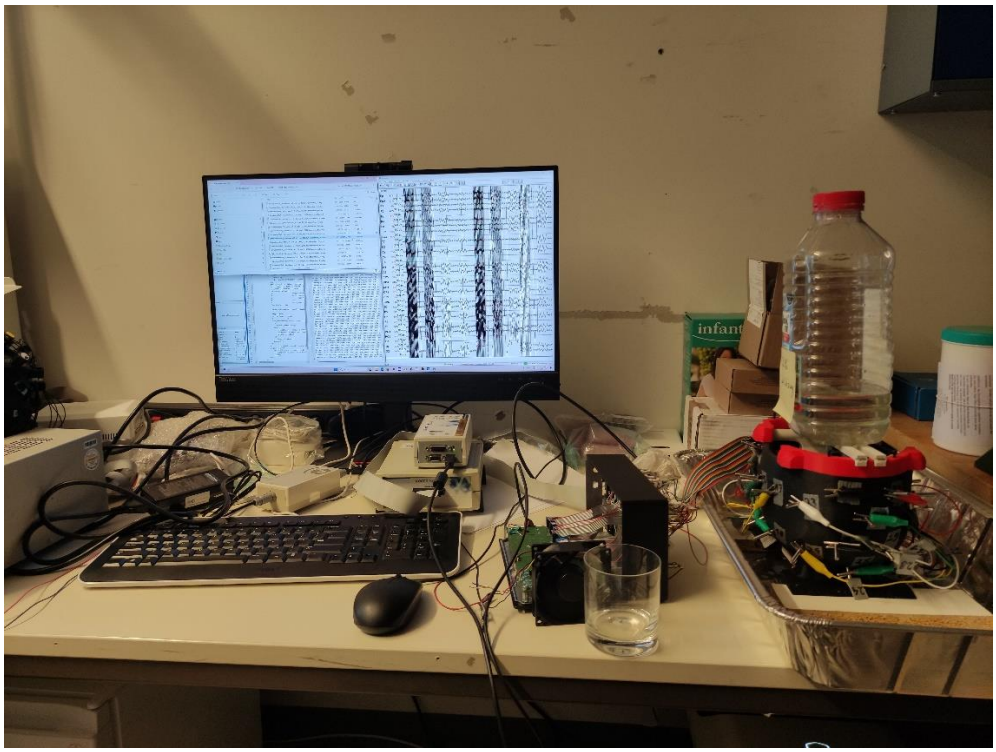

**Fig. 13:** Setup for measurement with skull and cortex and improvised weight

We tried to generate at least 8 frames for each setup of the tank: empty, skull and cortex. One frame for the possible combinations of frequencies 33Hz, 90Hz, 333Hz, 800Hz and amplitudes 4µA, 39µA. Each frame then contained all sink source electrode pair combinations. The length of a single electrode pair measurement was around 0.7s and was done with a sampling rate of 5000 sample / second.

### 2.2.3 Pythonic, Yet Rudimental, Electrical Impedance Tomography Expert (Pyreite)

Pyreite[15] is a small python based framework written by Nils Harmening that can be used to run a fast EIT measurement before an EEG experiment. It requires small hardware changes but offers improved source localization by providing conductivity estimates for different layers of the head. This was used in combination with OpenMEEG[16] to create the simulation used to compare the phantom recordings against.

### 2.2.4 Comparison

To prepare the measured EIT data for comparison we first applied a baseline correction followed by a Butterworth filter centered on the target frequency to reduce possible noise. This data is then used to calculate the root mean squared amplitude for each frame, which is used to compare different frames by calculating the correlation of the amplitudes. A similar thing was done to compare the simulations with the experiments. There we used

[15] Github link: https://github.com/harmening/pyreite

[16] Available here: https://openmeeg.github.io/

the Dirichlet matrix generated with Pyreite and calculated the correlation to the amplitudes.

# 3 Chapter – Results

## 3.1 Protopasta Conductivity trials

Given the conductivity from the official documentation[17] we were expecting values around 30 Ω*cm on x-y plane and 115 Ω*cm along the z-axis. There is no information regarding the infill percentage so it could go up.
Tab. 2 shows the average conductivity for the cube measurement without any silver paint added. It does not have all the infill ratios and only a single trial for these because the clamp to apply the pressure broke after some measurements.

**Tab. 2:** Shows the average conductivity in Ω*cm for the cubes without silver paint

| | x-axis (Ω*cm) | y-axis (Ω*cm) | z-axis (Ω*cm) |
|---|---|---|---|
| 5% infill - Honeycomb | 243 | 148,5 | 176 |
| 50% infill - Honeycomb | 103 | 107,5 | 192 |
| 100% infill - Honeycomb | 52,5 | 45 | 315 |
| 100% infill - Lines | 60 | 62,5 | 675 |

The data for the cubes with silver paint was 11 different infill ratios. (see **Error! Reference source not found.** and Fig. 15). We were focusing more on the lower ratios because at some point the conductivity should increase slower and we had the 100% infill ratio to compare against.
The data had more variance below 35% infill because they were the first to be measured and it could be that the silver paint was not completely dry or not applied correctly. If a cube had a resistivity higher than 150 Ω*cm, it often also took some time until this value was reached which seemed like the contact resistance was still too high. We then applied

[17] Available here: https://proto-pasta.com/pages/conductive-pla#CCcoductivity

another small layer of paint to these cubes until the results improved and were stable again.
The data shows that the conductivity of the x-y plane only improves slightly with an increase of the infill density and stays around 50 Ω*cm. The z-axis is affected by the increase and is able to nearly half its median resistivity from 93 Ω*cm at 5% infill to around 40 Ω*cm at 100% infill.

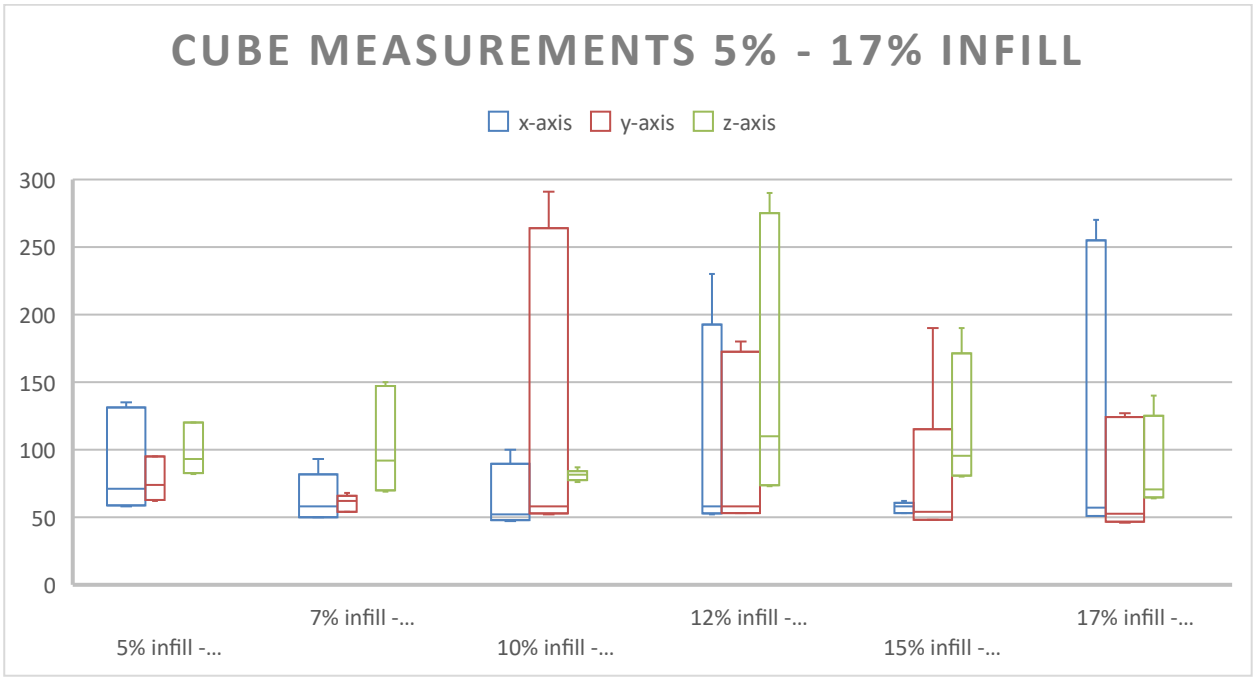


**Fig. 14:** Cube measurements 5% - 17% infill ratio

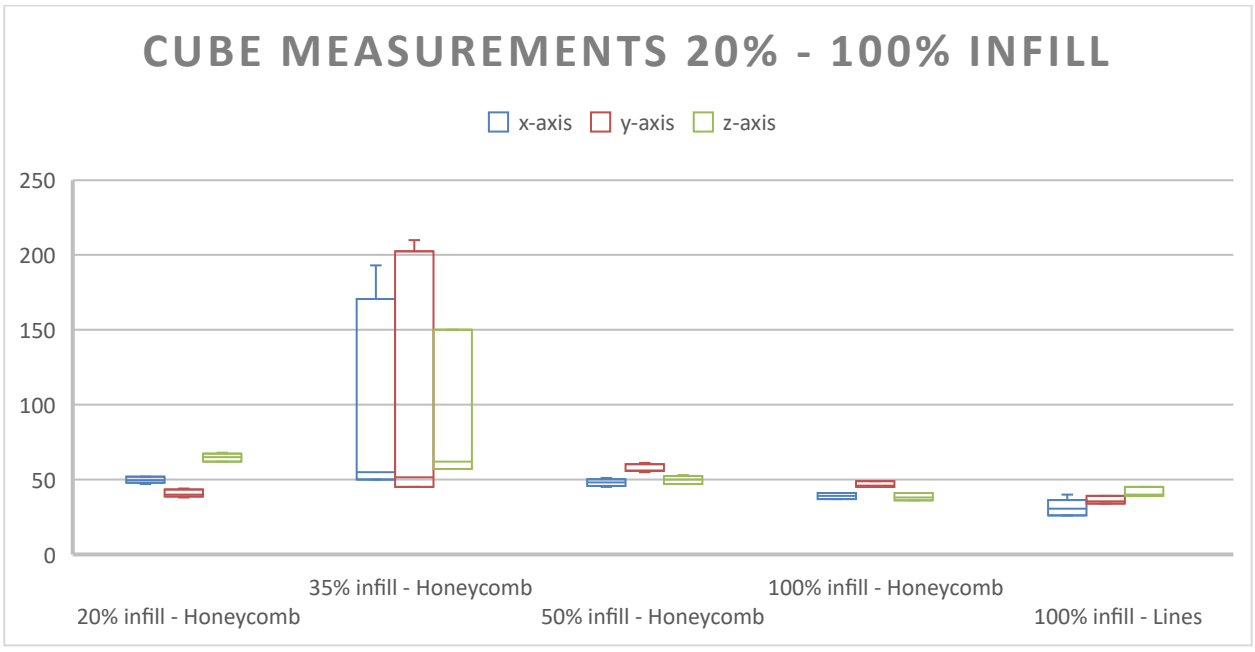


**Fig. 15:** Cube measurements 20% - 100% infill

Given this data we decided to use 50% honeycomb infill to print the cortex as all 3 axes have a similar conductivity and we would have enough PLA to print it because we only

had 500 g rolls of the conductive PLA. Before the actual print the slicer estimated that the cortex with 50% infill would require more than 500g. As a result we tried to remove some support structures and the raft. Which was not enough and we also had to reduce the infill flow rate by 10%-20% until the estimation was below the 500 g limit. During the first print of the cortex, the model would again not stick to the baseplate and we had to start again with less material. We estimated 20g as an upper limit of the material used for the failed print and had to adjust our settings to now stay below 480g and include a raft. We could reach this with an infill flowrate of 70%. Fig. 16 shows the resulting measurement and it was similar to the 10% flowrate. We took the average value of 65Ω*cm to generate the simulation with a cortex that was 4 times more conductive than reality.[18]

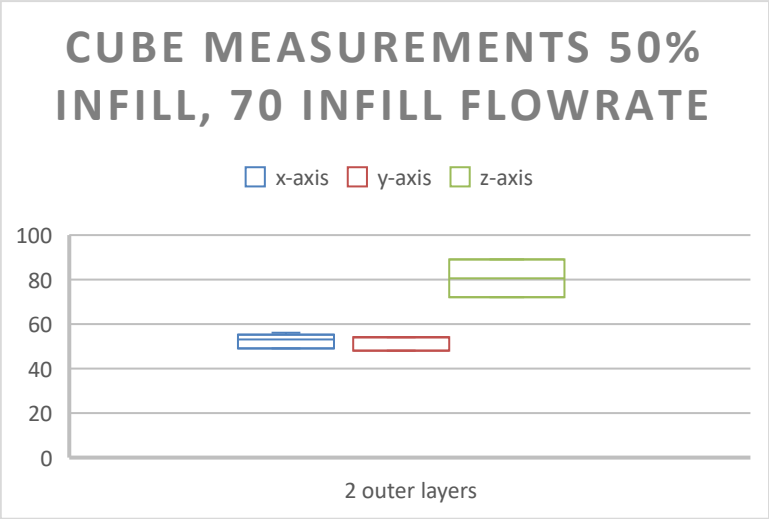


**Fig. 16:** Cube measurements for 50% infill and 70% infill flowrate.

## 3.2 Correlation between experimentation frames

### Hardware noise

To get an estimate of the hardware noise used the runs without anything in the tank. We compared the frames with the same frequency and amplitude settings from these runs. Tab. 3 shows that the lower frequencies all have a high average correlation, independent of the amplitude used. Starting with 300Hz the correlation drops a lot which was probably

[18] Raw data available here: https://tubcloud.tu-berlin.de/s/73Btzn8DikJYcTr

caused by the measurement device overheating and temporarily shutting down our first test session. For later runs the device was opened up and a PC fan was used to cool it.

**Tab. 3:** Correlation of frames without the skull and the same frequency, amplitude settings.

| Trial 1 | Trial 2 | Average correlation |
|---|---|---|
| 33 Hz, 4 µA | 33 Hz, 4 µA | 0.976 |
| 90 Hz, 4 µA | 90 Hz, 4 µA | 0.946 |
| 333 Hz, 4 µA | 333 Hz, 4 µA | 0.688 |
| 800 Hz, 4 µA | 800 Hz, 4 µA | 0.573 |
| 33 Hz, 39 µA | 33 Hz, 39 µA | 0.986 |
| 90 Hz, 39 µA | 90 Hz, 39 µA | 0.981 |
| 333 Hz, 39 µA | 333 Hz, 39 µA | 0.442 |
| 800 Hz, 39µA | 800 Hz, 39 µA | 0.469 |

### Influence of skull hole orientation

**This section focusses on the part of the work from (Avery J. a., 2017) that mentions the need to use different skulls for multifrequency EIT. To test, this we used the data generated with the skull and compared different frequencies (see Tab. 4 and**

Tab. 5). The frames with an amplitude of 4 µA show that the frequencies have an influence on the outcome. The greater the difference between two frequencies the lower the correlation. This effect is amplified with a higher amplitude.

**Tab. 4:** Correlation between frames with skull, different frequencies and an amplitude of 4 µA

| Frequency 1 | Frequency 2 | Average correlation |
|---|---|---|
| 33 Hz | 90 Hz | 0.962 |
| 33 Hz | 333 Hz | 0.868 |
| 33 Hz | 800 Hz | 0.795 |
| 90 Hz | 333 Hz | 0.877 |
| 90 Hz | 800 Hz | 0.799 |
| 333 Hz | 800 Hz | 0.814 |

**Tab. 5:** Correlation between frames with skull, different frequencies and an amplitude of 39 µA

| Frequency 1 | Frequency 2 | Average correlation |
|---|---|---|
| 33 Hz | 90 Hz | 0.964 |
| 33 Hz | 333 Hz | 0.411 |
| 33 Hz | 800 Hz | 0.239 |
| 90 Hz | 333 Hz | 0.433 |
| 90 Hz | 800 Hz | 0.258 |
| 333 Hz | 800 Hz | 0.467 |

### Skull with Cortex

Due to time constraints we only managed to gather data for 4 frames with different frequencies and an amplitude of 39 µA for the setup with skull and cortex. Additionally a fridge was interfering with the experiment. When it started to cool, the measuring device would sometimes disconnect from the PC. This was only discovered relatively close to the end.
The overall correlation is similar to the results without the cortex. It also decreases when the frequencies are further away from each other.

**Tab. 6:** Correlation between frames with skull + cortex, different frequencies and an amplitude of 39 µA

| Setting 1 | Setting 2 | Average correlation | Median |
|---|---|---|---|
| 33 Hz | 90 Hz | 0.866 | 0.998 |
| 33 Hz | 333 Hz | 0.424 | 0.217 |
| 33 Hz | 800 Hz | 0.243 | 0.110 |
| 90 Hz | 333 Hz | 0.463 | 0.317 |
| 90 Hz | 800 Hz | 0.266 | 0.127 |
| 333 Hz | 800 Hz | 0.354 | 0.249 |

## 3.3 Correlation with Simulation

Fig. 17 shows the correlation between the experiments and the simulations with an overall maximum correlation of 0.7. It is possible to see the effects of the overheating in the empty tank graph where the correlation drops to 0.4 and 0.2 for the higher frequencies for the first run. While it only slightly decreases in the second run. The results for the skull also very similar to the ones from the experimentations where the frequency and the amplitude have a strong effect on the correlation. Since we had to reduce the quality of the printed cortex we generated 3 different simulations where the conductivity of the cortex

was increased by the factors 4, 4.25 and 4.5. Surprisingly these factors seemed to make no difference at all.
The 39 µA graphs all had a common trend compared to the experiment where the hardware had heat problems which could mean that the fan was not enough to cool the measurement device. As shown in Fig. 17d.

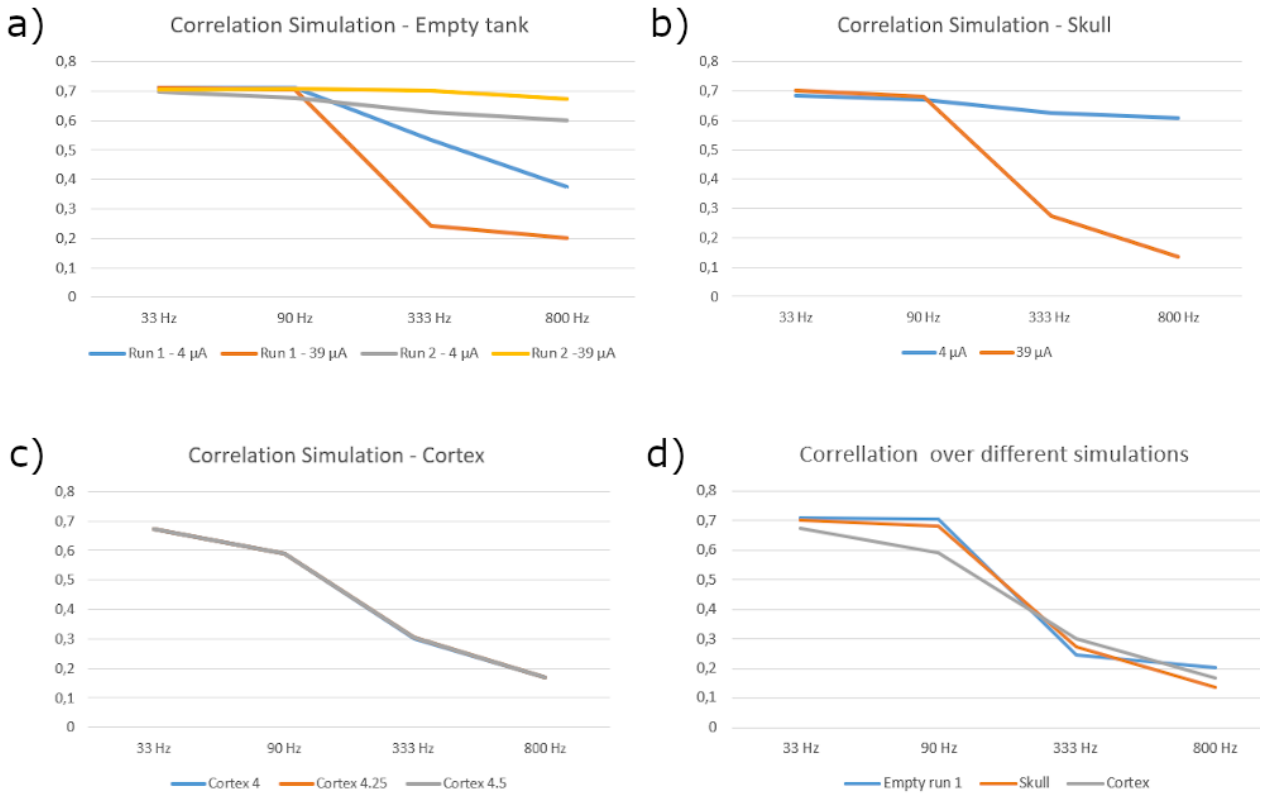


**Fig. 17:** Correlations between simulations and experiments. a) Empty tank b) Skull c) Skull + Cortex d) similar correlation trends

## 3.4 Discussion

Avery et al. succeeded in designing a phantom was easy to build and it didn’t take long until we were able to gather our first set of data.
Our hardware was relatively stable at lower frequencies but prone to overheating when performing experiments with higher frequencies. The added CPU fan seemed to fix this at first but looking at the results from the comparison with the simulations. It appeared that the increase in resistivity caused by the skull and cortex would push the hardware beyond its limits. There is also the small chance that the skull could be the reason for this. Since it was designed for 1kHz and we used it for all our frequencies. With the amount of data we had it was not possible to accurately determine the correct reason for this behavior.
Looking at the results of the simulations comparisons leads to the question why the maximum correlation is only 0,7 over all different experiments. A possibility for this could be noise introduced through low voltage electrodes as we did not exclude them data. But the trend of the correlations was always similar to experimentation results. Using the 33 Hz result as base and comparing it with the other frequencies.
Since the graphs in Fig. 17c are all identical and very similar it would seem that the conductivity of the cortex had no effect on the results or was completely overshadowed by the effect of the skull. This would make it also impossible to determine if the cortex works or not.
In general, we should have generated a lot more data, Avery et al. had at least 20 frames for similar setups and we had a maximum of 16 for the empty tank, 8 for the skull and only 4 for cortex. We should have spent more of the time to generate data for verification and comparison and possibly try to run this experiment on another hardware setup as well. However we also wanted to find a material that could be used to simulate the cortex and had some difficulties measuring the results.

As a positive note we were not the only ones experimenting with conductive PLA for EIT experiments. Creegan et al. were also experimenting with different infill ratios to create a dry EIT phantom (see Fig. 18). They were printing a disc with an overall high infill ratio and a small area where it was reduced. The disc was then surrounded by electrodes to

create a ring phantom. They were also using a custom EIT device for measuring. But their reconstruction was overall very accurate.
They had higher values for the infill to conductivity relationship. That could be caused by using a higher printing temperature which was not mentioned.

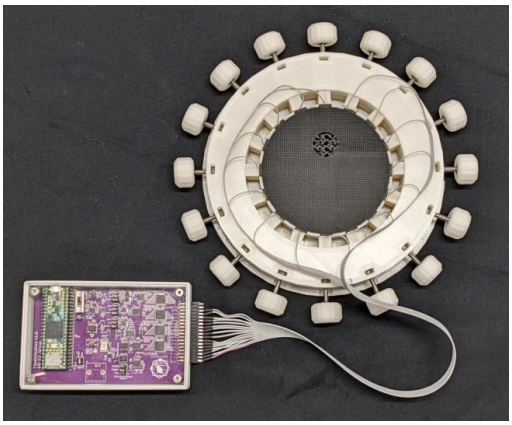

**Fig. 18:** Dry phantom using conductive PLA for reconstruction[19]

As an option for the future it would be interesting to see if it is possible to print a layered phantom with scalp, skull, cerebral spinal fluid and cortex as a ring. And if this works maybe a complete head shaped phantom. IdeaMaker would support this because it allows the import of meshes as modifiers. These modifier could then be used to set specific infill ratios in the area of the intersection.

[19] Adapted from Fig. 11 (Creegan, 2024)

# 4 Bibliography

Avery, J. a. (2017). A Versatile and Reproducible Multi-Frequency Electrical Impedance Tomography System. *Sensors*.

Avery, J., Aristovich, K., Low, B., & Holder, D. (2017). Reproducible 3D printed head tanks for electrical impedance tomography with realistic shape and conductivity distribution. *Physiol. Meas., 38*, 1116. doi:10.1088/1361-6579/aa6586

Bera, T. K., Chowdhury, A., Mandai, H., Kar, K., Haider, A., & Nagaraju, J. (2015). Thin domain wide electrode (TDWE) phantoms for Electrical Impedance Tomography (EIT). *Proceedings of the 2015 Third International Conference on Computer, Communication, Control and Information Technology (C3IT)*, (pp. 1-5). doi:10.1109/C3IT.2015.7060223

Creegan, A. N. (2024). A novel two-dimensional phantom for electrical impedance tomography using 3D printing. *Scientific Reports*, 2115.

Gurunathan, T. R. (2013). Polyurethane conductive blends and composites: synthesis and applications perspective. *Journal of Materials Science*, 67–80.

H. Gagnon, M. C. (2010). A Resistive Mesh Phantom for Assessing the Performance of EIT Systems. *IEEE Trans. Biomed. Eng., 57*, 2257--2266. doi:10.1109/TBME.2010.2052618

Jun Ogata, I. F. (1973). The Relative Weight of the Gray and White Matter of the Normal Human Brain. *Journal of Neuropathology & Experimental Neurology*, 585–588.

Khalid, I. (2023). A Brief Study of Methods to Determine the Electrical Resistivity of Materials. *Indonesian Journal of Applied Physics*, 53.

Kim, Y. H. (2016). Ultrasound Phantoms to Protect Patients from Novices. *The Korean journal of pain vol. 29*, 73-77.

Li, J.-B. a.-T.-H.-S.-X.-Z. (2014). A New Head Phantom With Realistic Shape and Spatially Varying Skull Resistivity Distribution. *IEEE Transactions on Biomedical Engineering, 61*, 254-263.

Li, J.-B., Tang, C., Dai, M., Liu, G., Shi, X.-T., Yang, B., . . . Dong, X.-Z. (2014). A New Head Phantom With Realistic Shape and Spatially Varying Skull Resistivity

Distribution. *IEEE Transactions on Biomedical Engineering, 61*, 254-263. doi:10.1109/TBME.2013.2288133

Marie Wegner, E. G. (2023). Classification of phantoms for medical imaging. *Procedia CIRP, 119*, 1140-1145. doi:https://doi.org/10.1016/j.procir.2023.03.154

McCann H, P. G. (2019). Variation in Reported Human Head Tissue Electrical Conductivity Values. *Brain topography*, 110-115.

Melo, D. S. (2023). Evaluation of Piezoresistive and Electrical Properties of Conductive Nanocomposite Based on Castor-Oil Polyurethane Filled with MWCNT and Carbon Black. *Materials*.

Miklody, D. (2014). *Refining Source Localization Through Bioimpedance Measurements.* (Master thesis) Technische Universität Berlin, Berlin.

Owda, A. Y., & Casson, A. (2021, jul). Investigating Gelatine Based Head Phantoms for Electroencephalography Compared to Electrical and Ex Vivo Porcine Skin Models. *IEEE Access, 9*, 96722--96738. doi:10.1109/ACCESS.2021.3095220

Saeid Mehvari, B. G.-V. (2023). Effect of processing methods on the electrical conductivity properties of silver-polyurethane composite films (Experimental and numerical studies). *Journal of Composite Materials*, 4409–4422.

Takhti, M., & Odame, K. (2019). Structured Design Methodology to Achieve a High SNR Electrical Impedance Tomography. *IEEE Trans. Biomed. Circuits Syst.*, 364--375.

Tang, C. a. (2008). Correlation Between Structure and Resistivity Variations of the Live Human Skull. *IEEE Transactions on Biomedical Engineering*, 2286-2292.

Tidswell AT, B. A. (2003). A comparison of headnet electrode arrays for electrical impedance tomography of . *Physiological measurement*, 527-44.

Tom Tidswell, A. G. (2001). Three-Dimensional Electrical Impedance Tomography of Human Brain Activity. *NeuroImage*, 283-294.

Yu, F.-M. a.-N.-W.-Y. (2006). A Rotative Electrical Impedance Tomography Reconstruction System. *Journal of Physics: Conference Series*, 542.

Zarafshani, A., Qureshi, T., Bach, T., Chatwin, C., & Soleimani, M. (2016). A 3D multi-frequency response electrical mesh phantom for validation of the planar structure EIT system performance. In *IEEE International Conference on Electro Information Technology (EIT)* (pp. 19--21). IEEE.

Zhang, J., Yang, B., Li, H., Fu, F., Shi, X., Dong, X., & Dai, M. (2017). A novel 3D-printed head phantom with anatomically realistic geometry and continuously varying skull resistivity distribution for electrical impedance tomography. *Scientific reports, 7*, 4608.